Modeling of Critical Cutting Speed of White Layer Formation in Hard-Cutting Process

Zhang Fangyuan (zhangfangyuan@nbu.edu.cn)
Ningbo University
Li Kai
Ningbo University
Duan Chunzheng
Dalian University of Technology

Research Article

Keywords: Hard-Cutting, White Layer, Critical cutting speed, Austenite transformation driving force model

Posted Date: June 29th, 2021

DOI: https://doi.org/10.21203/rs.3.rs-639656/v1

Modeling of critical cutting speed of white layer formation in hard-cutting process

Zhang Fangyuan*[a], Li Kai [a], Duan Chunzheng [b]

a Faculty of Mechanical Engineering, Ningbo University, Ningbo 315211, China

b School of Mechanical Engineering, Dalian University of Technology, Dalian 116024, China

Email: zhangfangyuan@nbu.edu.cn

Abstract: White layer exists on the machined surface of the hard-cutting and affects the surface quality and mechanical properties of a workpiece. Accurate predicting the critical cutting speed of white layer formation is of great significance for controlling the surface quality and selecting appropriate cutting parameters. In this work, an austenite transformation driving force calculation model of the white layer formation was established based on phase transformation thermodynamics theory, in which the influence of cutting temperature, stress and strain on the austenite transformation driving force in the hard-cutting process was taken into account. Second, a finite element (FE) model of the hard-cutting process was built by using hardened AISI52100 steel as cutting material. Then, a prediction model of critical cutting speed of the white layer formation was developed in combination with the austenite transformation driving force model and the hard-cutting FE model. Finally, the critical cutting speeds of the white layer formation at different chip thicknesses, tool rake angles and different levels of flank wear were simulated by using the critical cutting speed prediction model.

Key Words: Hard-Cutting; White Layer; Critical cutting speed; Austenite transformation driving force model

0 Introduction

Hard-cutting, which has advantages of high quality, high efficiency and environmental protection, is being widely used in finishing hardened steel. However, workpiece is subjected to extremely high temperature and severe plastic deformation as the result of high hardness, which inevitably leads to the dramatic changes in the machined surface. Scholars has observed that white layer is formed on the machined surface during hard-cutting process[1] and differ from the bulk material in microstructure[2], surface quality[3] and mechanical property[4]. The white layer has complex effects on the performance of the workpiece[5], it is desirable to be produced in some cases[6], yet not in others[7, 8]. Therefore, modeling a critical cutting speed of white layer formation in the hard-cutting process is of vital importance for controlling the formation of the white layer and selecting reasonable cutting parameters.

In recent years, the properties and formation mechanism of the white layer have been explored in detail. The crystalline grain of the white layer is refined seriously, the hardness as well as the retained austenite content are higher than those of bulk material [9]. Chou and Evans [10] observed the white layer morphology in the hard turning of AISI52100 steel. They considered that the formation of the white layer is dominated by a rapid heat–cooling process, and cutting heat causes austenite and martensite transformations. Du et al.[11] analyzed the white layer of Ni based powder superalloy induced by cutting process, and found that phase transformation white layer can be observed when the cutting temperature is lower than the phase transformation temperature. They indicated that plastic deformation promotes the formation of the white layer. Zhang et al. [3, 12] studied the formation mechanism of the white layer of AISI52100. The experimental results demonstrated that the white layer is formed by phase transformation, and plastic deformation provides the phase transformation driving force, which accelerates the formation of the white layer.

Experimental research has indicated that the white layer is induced by phase transformation in some cutting conditions[12, 13]. It is of great significance to predict the white layer based on its properties and formation mechanism. In recent years, scholars have carried out in-depth exploration on the prediction of the white layer, in which the prediction model of white layer thickness is the most studied. Chou et al.[10] developed an empirical model based on the moving heat source. The model used the heat generated by plastic deformation and friction as moving heat source to calculate the temperature of the machined surface. If the machined surface temperature exceeds phase transformation temperature, the white layer is considered to be formed. Umbrello et al.[14] established a FE prediction model of the white layer thickness in dry hard-cutting process based on a hardness criterion. When the hardness of the machined surface exceeds matrix hardness, the white layer is determined to be produced.

Stress and strain have influence on the phase transformation temperature of the white layer[15], and thus, some scholars believed that the calculation model of the white layer thickness needs to be built on the basis of considering the effects of stress and strain. The influence of stress on austenite transformation temperature were taken into account by Ramesh et al., and the white layer thickness was predicted by using FE method[16]. Kong et al.[17] considered the effects of alloy elements, stress and strain on the phase transformation temperature of the white layer and established a critical austenite transformation temperature model of the white layer based on the phase transformation free energy theory. Then, the model was combined with a hard-cutting FE model to predict the thickness of phase transformation white layer at different cutting parameters. Zeng et al. [18] established a

prediction model for white layer thickness based on phase transformation mechanism as well, the effects of stress, elastic and plastic strain on phase transformation temperature were considered.

Although some investigations into the modeling of the white layer in hard-cutting process were reported, certain problems have not been resolved. First, the research on the theoretical modeling of the white layer mainly focuses on the prediction of the white layer thickness. Nevertheless, the prediction of critical cutting speed of the white layer formation has not been studied in detail, yet establishing a model of critical cutting speed of the white layer formation has a guiding role in selecting reasonable cutting parameters. Second, driving force of austenite phase transformation plays significant roles in the white layer formation in the hard-cutting process. The kinetics of austenite formation involved in previous studies mainly focused on the heat treatment processes[19–21]. Nevertheless, plastic deformation was not included in these kinetics models, which has deeply influence on the formation of white layer. Therefore, stress and strain should be taken into account when calculating the austenite phase transformation driving force. Next, stress and strain cannot be measured in the process of cutting experiments, however, hard-cutting FE model can simulate these parameters accurately. Accordingly, combining the austenite phase transformation driving force model with the hard-cutting FE model to predict the critical cutting speed is worthy of study.

Accordingly, the following studies were carried out. A driving force model of the white layer austenite transformation was established based on the free energy change principle, and the influence of cutting temperature, stress and strain on the driving force were considered in the model. Then, a hard-cutting FE model was developed to simulate the cutting temperature, stress and strain distribution of the hard-cutting workpieces. Next, a critical cutting speed model of the white layer formation was established by combining the driving force model with the hard-cutting FE model. The critical cutting speed of the white layer formation calculated by the theoretical model was compared with the cutting experimental results. At last, the influences of cutting parameters, rake angle and different levels of flank wear on the critical cutting speed of the white layer formation were predicted and discussed.

1 Calculation model of austenite phase transformation driving force in hard-cutting process

Research by Zhang et al.[3] indicated that the retained austenite volume of the white layer is higher than that of the bulk material, demonstrating that austenite transformation occurs in the hard-cutting process. In the hard-cutting process, phase transformation white layer is induced by solid phase transformation. Free-energy

change ΔG in metal solid transformation process is determined by phase transformation driving force and resistance. The solid phase transformation cannot be carried out unless ΔG <0, i.e. the phase transformation driving force is greater than the phase transformation resistance. High cutting temperature and plastic deformation provide the driving force for the white layer formation[22].

2.1 Driving force of austenite transformation provided by cutting temperature

Kooiker et al. [23] established a martensite to austenite reversion model and demonstrated that temperature is one of the main factors affecting the austenite transformation process. In the white layer austenitizing process, martensite M is parent phase, and austenite γ is new phase. Fig. 1 shows the tendency of martensite and austenite free energy with temperature. The martensite cannot be transformed to the austenite unless molar free energy of austenite is lower than that of the martensite:

$$\Delta G_V^{M\to\gamma} = G_\gamma - G_M < 0 \tag{1}$$

where, $\Delta G_V^{M\to\gamma}$ is austenite transformation driving force induced by cutting temperature (J/mol), G_γ is molar free energy of austenite (J/mol), G_M is molar free energy of martensite (J/mol). At the austenite equilibrium transformation temperature A_{cm}, $\Delta G_V^{M\to\gamma}$ = 0. However, austenite transformation cannot be carried out in this case. When the cutting temperature is higher than A_{cm}, $\Delta G_V^{M\to\gamma}$ < 0, driving force can be provided by cutting temperature and promote the austenite transformation.

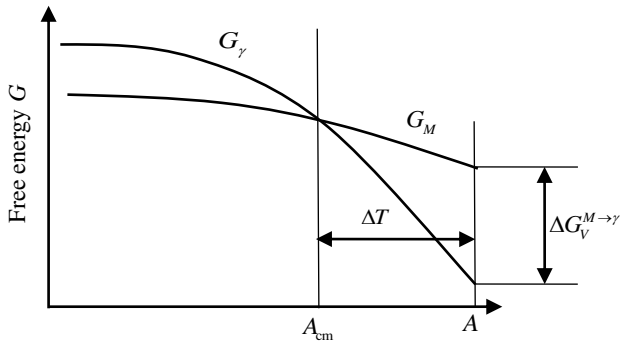

Fig. 1 Tendency of martensite and austenite free energy with temperature

The free energy of a substance is given by [24]:

$$G = H - TS \tag{2}$$

where, H is molar enthalpy (J/mol), S is molar entropy (J/(mol·K)), T is temperature (K).

The free energy, enthalpy and entropy of a system change with temperature. In the constant-pressure process, molar enthalpy change ΔH due to temperature is written as [25]:

$$\Delta H=\int_{T_1}^{T_2} C_P(T)\,dT \tag{3}$$

where, $C_P(T)$ is molar heat capacity at constant pressure (J/(mol·K)).

Molar entropy change ΔS due to temperature is [25]:

$$\Delta S=\int_{T_1}^{T_2} \frac{C_P(T)}{T}dT \tag{4}$$

Through regression analysis of experimental data, the relationship between the $C_P(T)$ and temperature is described by a polynomial relation [25]:

$$C_P(T)=a+bT+cT^2 \tag{5}$$

where, a, b, c are constants, the values of a, b, c of martensite and austenite are shown in Tab. 1.

Tab. 1 Parameters of molar heat capacity [25]

Phase	a	b	c
Martensite	17.49	24.77×10^{-3}	0
Austenite	26.61	6.28×10^{-3}	0

Then the expressions of H and S were obtained by integrating the Eqs.3 and 4:

$$H=H(298\mathrm{K})+\int_{298\mathrm{K}}^{T_2} C_P(T)dT \tag{6}$$

$$S=S(298\mathrm{K})+\int_{298\mathrm{K}}^{T_2} \frac{C_P(T)}{T}dT \tag{7}$$

where, $H(298\mathrm{K})$ and $S(298\mathrm{K})$ are the molar enthalpy and molar entropy at the temperature of 298K. The $H(298\mathrm{K})$ and $S(298\mathrm{K})$ of martensite and austenite are shown in Tab. 2.

Tab. 2 Molar enthalpy and molar entropy of austenite and martensite at 298K[25]

Phase	$H(298\mathrm{K})$ (J/mol)	$S(298\mathrm{K})$ (J/(mol·K))
Martensite	0	27.28
Austenite	6.78	33.66

Combining Eq. 5 with Eqs.6-7, and substituting the data in Tabs 1-2 into Eqs.6 - 7, one obtains the change rule of H and S due to temperature:

$$H^M=17.49T+12.385\times10^{-3}T^2-6312 \tag{8}$$

$$S^M=17.49\ln T+24.77\times10^{-3}T-83 \tag{9}$$

$$H^\gamma=26.61T+3.14\times10^{-3}T^2-1428.62 \tag{10}$$

$$S^{\gamma} = 26.61\ln T + 6.28\times10^{-3}T - 119.81 \tag{11}$$

where, H^{M}, H^{γ} and S^{M}, S^{γ} mean the molar enthalpy and entropy of martensite and austenite, respectively.

Combination of Eqs.1-2 to the following relations:

$$\Delta G_V^{M\to\gamma} = G^{\gamma}\text{-}G^{M} = H^{\gamma} - TS^{\gamma} - (H^{M} - TS^{M}) = \Delta H^{M\to\gamma} - T\Delta S^{M\to\gamma} \tag{12}$$

After substituting Eqs.8-11 into Eq.12, $\Delta G_V{}^{M\to\gamma}$ can be given as:

$$\Delta G_V{}^{M\to\gamma} = 45.93T + 9.245\times10^{-3}T^2 - 9.12T\ln T + 4883.38 \tag{13}$$

So far, the calculation model of austenite transformation driving force provided by cutting temperature was established. When $\Delta G_V{}^{M\to\gamma}$=0, the free energy of martensite is equal to that of austenite. On $\Delta G_V{}^{M\to\gamma}$ being less than 0, the molar free energy difference between austenite and martensite begins to provide driving force for $M\to\gamma$ transformation.

2.2 Driving force of austenite transformation provided by stress and strain

In the hard-cutting process, the white layer formation is affected by both plastic deformation and cutting temperature. Ramesh et al[16] investigated the influence of stress and strain on the austenite equilibrium transformation temperature A_{cm}, and found that high stress and strain cause a decrease in A_{cm}, which demonstrated that austenite transformation driving force can be provided by the plastic deformation in the hard-cutting process.

According to the thermodynamic principles of phase transformation, the free energy change due to stress P at constant temperature T:

$$\Delta G_T = \int_{P_1}^{P_2} V dP \tag{14}$$

where, ΔG_T is free energy change induced by stress (J/mol), V is molar volume of a substance (m^3/mol).

As the molar volume of martensite differs from that of austenite, the ΔG_T cannot be calculated by Eq. 14 directly. However, the free energy is state variable, ΔG_T is only related to the initial and final state of the system, but not to the process. Therefore, ΔG_T caused by pressure can be expressed by:

$$\Delta G_T{}^{M\to\gamma} = \left(V_{\gamma} - V_M\right)(P - P_0) = \Delta V^{M\to\gamma}(P - P_0) \tag{15}$$

$\Delta V^{M\to\gamma}$ is molar volume increment from martensite to austenite, P is compressive stress on the machined surface caused by the cutting process (Pa), P_0 is the stress on the surface before cutting process, which is atmospheric

pressure. The stress produced by the hard-cutting process is much larger than atmospheric pressure, and thus, it is assumed $P_0 = 0\text{Pa}$.

The molar mass of iron is $55.85\ \text{g/mol}$, the densities of austenite and martensite are $7.633\ \text{g/cm}^3$ and $7.571\ \text{g/cm}^3$, respectively. Therefore, the molar volume increment from martensite to austenite is shown as follows:

$$\Delta V^{M\to\gamma} = \frac{55.85\text{g/mol}}{7.633\times10^{-6}\text{g/m}^3} - \frac{55.85\text{g/mol}}{7.571\times10^{-6}\text{g/m}^3} = -0.06\times10^{-6}\,\text{m}^3/\text{mol} \tag{16}$$

Combining Eqs.15-16, then the free energy change of austenite transformation affected by stress can be obtained:

$$\Delta G_T^{M\to\gamma} = -0.06\times10^{-6}P \tag{17}$$

When a workpiece is deformed, the work done by the external force is transformed into strain energy W_S and stored in the workpiece. Then the external force decreases gradually, the strain energy storage caused by elastic deformation is released, which provides driving force for phase transformation. The strain energy in a micro-element is expressed as:

$$dW_S = \frac{1}{2}(\sigma_1 dydz)(\varepsilon_1 dx) + \frac{1}{2}(\sigma_2 dxdz)(\varepsilon_2 dy) + \frac{1}{2}(\sigma_3 dxdy)(\varepsilon_3 dz) = \frac{1}{2}(\sigma_1\varepsilon_1 + \sigma_2\varepsilon_2 + \sigma_3\varepsilon_3)(dxdydz) \tag{18}$$

Because the strain energy W_S can be obtained by the hard-cutting FE model, its value is directly extracted from the post-processing results of the FE model instead of establishing its calculation model.

Therefore, the driving force of austenite transformation induced by cutting temperature, stress and strain is described as:

$$\Delta G^{M\to\gamma} = \Delta G_V^{M\to\gamma} + \Delta G_T^{M\to\gamma} + W_S \tag{19}$$

$$\Delta G^{M\to\gamma} = 45.93T + 9.245\times10^{-3}T^2 - 9.12T\ln T + 4883.38 - 0.06\times10^{-6}P + W_S \tag{20}$$

Where, the unit of W_S is J/mol.

2 FE modeling of hard-cutting process

According to the established model, the driving force of austenite transformation of the white layer is affected by cutting temperature, stress and strain. The stress P and strain energy W_S cannot be measured directly during the cutting process, however, a hard-cutting FE model can predict the thermodynamic behavior in the machining process accurately. Therefore, an orthogonal cutting FE model was established by using ABAQUS

software. In the orthogonal cutting process, the material is in the state of plane strain, and thus, a two-dimensional rather than three-dimensional orthogonal cutting FE model was established, as shown in Fig. 2.

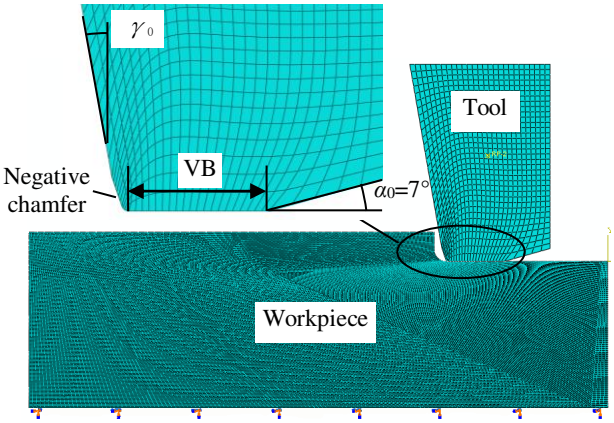

Fig. 2 FE model of orthogonal cutting

The material selected for the FE model was AISI52100 steel with the hardness of 60HRC. A Johnson-Cook (J-C) constitutive model was applied to describe the flow behavior of the hardened AISI52100. The J-C model coefficient and physical properties of the hardened AISI52100 steel are shown in Tabs. 3-4. The tool geometry and the cutting parameters are revealed in Tab. 5. The arbitrary Lagrange-Euler (ALE) approach was employed in the model, and the chip formation process was simulated via adaptive meshing. Therefore, the chip separation criterion is not needed in the orthogonal cutting model. The detailed establishing and verifying model process had been expressed in detail in our previous work ,which can be achieved in Ref [3].

Tab. 3 J-C model coefficient of AISI52100 steel [26]

Parameter	*A* (MPa)	*B* (MPa)	*C*	*n*	*m*
Value	1712	408	0.021	0.391	1.21

Tab. 4 Physical properties of AISI 52100 steel [17]

Temperature (°C)	Young's modulus (GPa)	Poisson's ratio	Expansion ($\times 10^{-6}$/(°C)	Conductivity(W /(m(°C))
22	201.0	0.277	11.5	52.5
200	179.0	0.269	12.6	47.5
400	163.0	0.255	13.7	41.5
600	103.0	0.342	14.9	32.5
800	86.9	0.396	15.3	26.0
1000	67.0	0.490	15.3	29.0
1500			14.9	30.0
Temperature ((°C)	Specific heat (J (kg/(°C))	Density (kg /m^3)		
25	458			
200	640	7827		
430	745			
540	798			

Tab. 5 Tool geometry and the cutting parameters

Rake angle (γ_0)	-10°, 0°, 10°
Relief angle (α_0)	7°
Flank wear (VB)	0mm, 0.1mm, 0.2mm
Cutting speed (v)	28m/min~550m/min
Chip thickness (a_c)	0.05mm, 0.1mm, 0.15mm

3 Modeling of critical cutting speed of white layer formation

3.1 Scheme of predicting critical cutting speed of the white layer formation

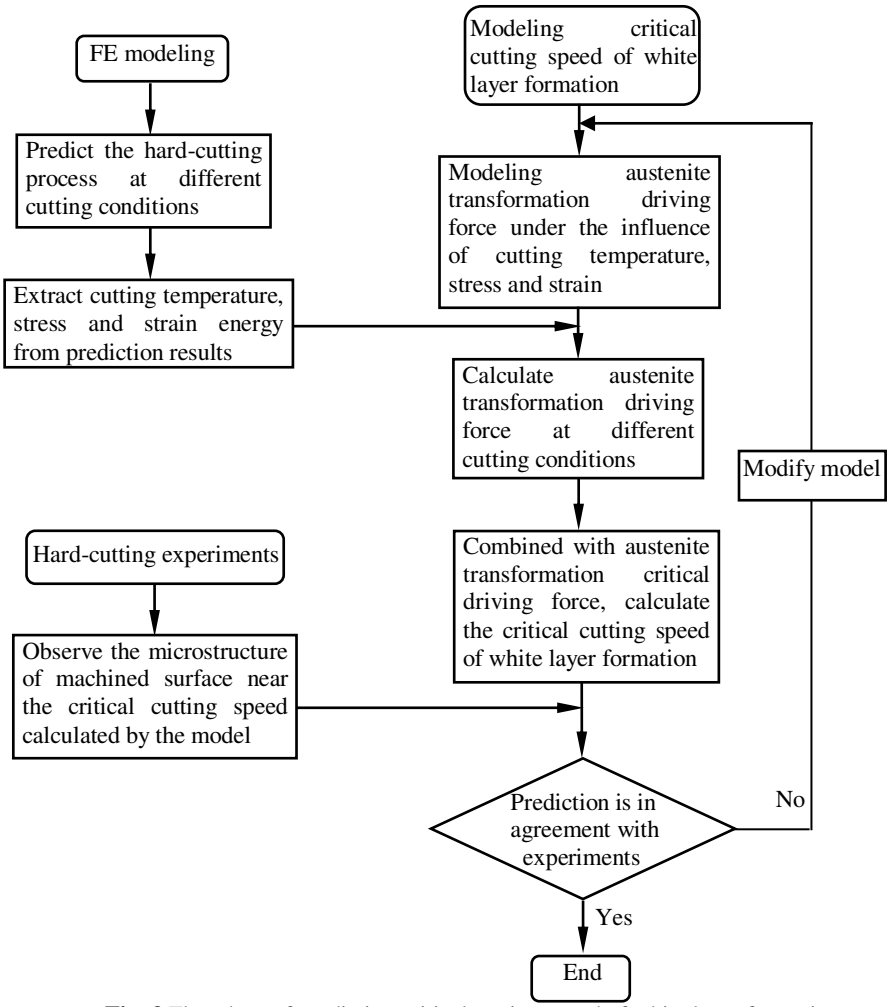

Fig. 3 Flowchart of predicting critical cutting speed of white layer formation

Combining the hard-cutting FE model with the austenite transformation driving force model, a critical cutting speed prediction model of the white layer formation was established. The flowchart is shown in Fig. 3. First, the austenite transformation driving force model under the influence of cutting temperature, stress and strain was established. The modeling process is described in Section 1.1. Second, the temperature, stress and strain energy data are extracted from the FE model and imported into the austenite transformation driving force model to

calculate the austenite transformation driving force at different cutting conditions. Then, the critical cutting speed of austenite transformation is determined by comparing the austenite transformation driving force provided by the hard-cutting process with the critical driving force of austenite transformation. Finally, verify the accuracy of the model. If the white layer cannot be observed in the machined surface at the cutting speed lower than the critical cutting speed predicted by the model, and can be observed at the cutting speed higher than the critical cutting speed, it is considered that the model can accurately predict the critical cutting speed of the white layer formation.

The critical cutting speed model cannot fully consider the factors which affect the austenite transformation in the white layer owing to the complicacy of this process. Therefore, the prediction model was appropriately simplified and the following basic assumptions were made:

① The workpiece is free of impurities after heat treatment and the influence of cementite on the austenite transformation driving force is ignored.

② When the austenite transformation driving force provided by the hard-cutting process reaches the critical driving force, it is considered that austenite transformation can occur in the machined surface.

3.2 Extraction of cutting temperature, stress and strain energy

This model aims to predict the critical cutting speed of the white layer formation, therefore, only the data of the top surface of the workpiece were extracted to calculate the driving force and the subsurface was not considered. The data extraction position is the contact point between the tool tip and the machined surface, as shown in Fig. 4.

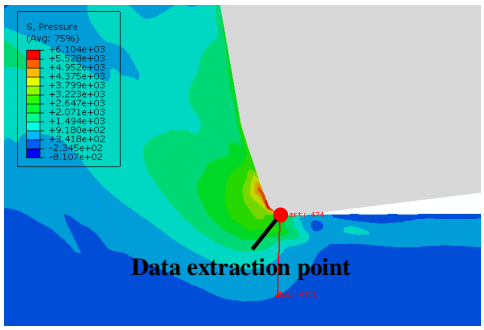

Fig. 4 Position of FE simulation data extraction

3.3 Calculation of critical cutting speed of the white layer formation

After the data of T, P and W_S extracting from the FE simulation results, $\Delta G^{M\to\gamma}$ was calculated through Eq.20. The temperature, stress, strain energy as well as the $\Delta G^{M\to\gamma}$ at different cutting speeds (γ_0 = -10°, a_c = 0.1mm, VB = 0 mm) are shown in Tab. 6.

Khodabakhshi et al. [27] measured the change of free energy in the austenite transformation process of carbon steel. The result showed that the free energy required for austenite transformation of carbon steel is 1156 J/mol, that is to say, the critical austenite transformation driving force is 1156 J/mol. The austenite transformation driving force calculated at different cutting speeds (γ_0 = -10° , a_c = 0.1mm, VB = 0 mm) was compared with the critical austenite transformation driving force, as shown in Fig. 5. At the cutting speeds of 28 m/min and 44 m/min, the austenite transformation driving force provided by the hard-cutting process is lower and higher than the critical austenite transformation driving force, respectively, which indicates that the white layer cannot and can be formed in the machined surface at these two cutting speeds. At the critical cutting speed, the austenite transformation driving force is equal to the critical austenite transformation driving force, and the critical cutting speed of white layer formation was determined by linear fitting method, which is 38m/min.

Tab. 6 FE prediction data and $\Delta G^{M\to\gamma}$ at different cutting speeds (γ_0 = -10°, a_c =0.1mm, VB = 0 mm)

v (m/min)	T (K)	P (MPa)	W_S (J/mol)	$\Delta G^{M\to\gamma}$ (J/mol)
28	720	1882	-158	-731
44	784	2123	-202	-1409
56	816	2262	-291	-1798
100	932	2753	-323	-2884
150	1003	3108	-332	-3479
200	1067	3523	-356	-4001
250	1187	3944	-360	-4803
300	1202	4026	-364	-4898
350	1237	4212	-368	-5104
400	1242	3566	-201	-4924
450	1248	3365	-184	-4926
500	1255	3195	-162	-4930
550	1259	3036	-113	-4892

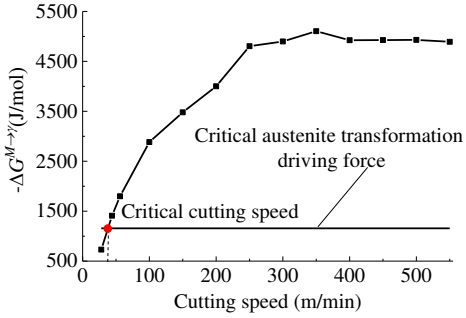

Fig. 5 Prediction of the critical cutting speed of white layer formation (γ_0 = -10° , a_c = 0.1mm, VB = 0 mm)

3.4 Model validation

To verify the accuracy of the simulation model, the predicted critical cutting speed were compared with the experimental results. The cutting experiments were performed in a MULTUS B400-W machining center, and the

set-up of the hard-cutting experiments is shown in Fig. 6. The hard-cutting experiments were carried out at the cutting speeds of 28m/min, 34m/min and 44m/min (γ_0 = -10° , a_c = 0.1mm, VB = 0mm). The material and cutting tool used in the experiments are consistent with those in the FE model. The machined surfaces were observed by Scanning Electron Microscope (SEM), as shown in Fig. 7. Figs. 7 (a) and (b) indicate that only plastic deformation layer caused by the hard-cutting process is observed in the machined surface at the cutting speeds of 28m/min, 34m/min, and no white layer is produced. However, white layer with the thickness of less than 1μm is observed in the machined surface at the cutting speed of 44m/min, as shown in Fig. 7 (c). The experiments indicated that the critical cutting speed of the white layer formation is between 34 m / min and 44 m/ min. The critical cutting speed predicted by the model is 38 m/ min, which is within the range of the experimental result. Therefore, it can be demonstrated that the established model can predict the critical cutting speed of the white layer formation accurately.

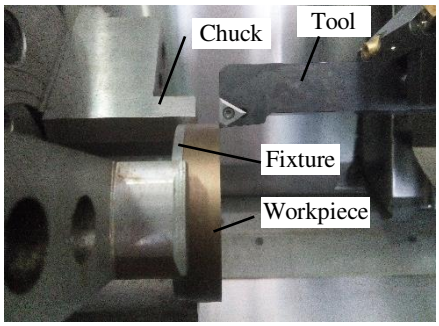

Fig. 6 Set-up of hard-cutting experiments

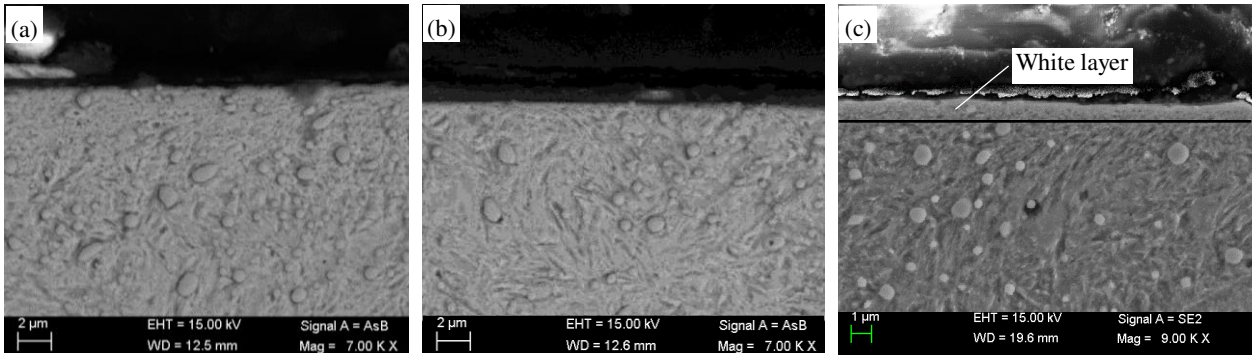

Fig. 7 SEM images of the machined surfaces at (a)v=28 m/min; (b)v=34 m/min; (c)v=44 m/min (VB = 0 mm, a_c = 0.1 mm)

4 Prediction of critical cutting speed of white layer formation in hard-cutting process

The austenite transformation driving force model demonstrates that cutting temperature, stress and strain all affect the white layer formation, while the cutting conditions, such as chip thickness, tool angle and tool wear, have influence on the cutting temperature and plastic deformation of the machined surface, thus affecting the

critical cutting speed of the white layer formation. As a result, the influences of cutting conditions on the critical cutting speed of the white layer formation were predicted and discussed.

4.1 Influence of chip thickness on the critical cutting speed of the white layer formation

The austenite phase transformation driving forces $\Delta G^{M\to\gamma}$ at different chip thicknesses (VB = 0 mm, γ_0 = -10°) were calculated and shown in Fig. 8 (a). It is noted that $\Delta G^{M\to\gamma}$ increases with the chip thickness at the same cutting speed. The cutting temperature, stress and strain energy of the machined surface increase with the chip thickness, which results in the increase in $\Delta G^{M\to\gamma}$. When the chip thickness is 0.15 mm, the $\Delta G^{M\to\gamma}$ exceeds the critical austenite phase transformation driving force at the cutting speed of 35 m/min, which indicates the white layer is formed at this cutting speed. The critical cutting speeds of the white layer formation at different chip thicknesses were predicted by using the critical cutting speed prediction model, as shown in Fig. 8 (b). The critical cutting speeds are 40.2 m/min, 38 m/min and 34.5 m/min at the chip thicknesses of 0.05 mm, 0.1 mm and 0.15 mm, which decrease slowly with the increase of chip thickness.

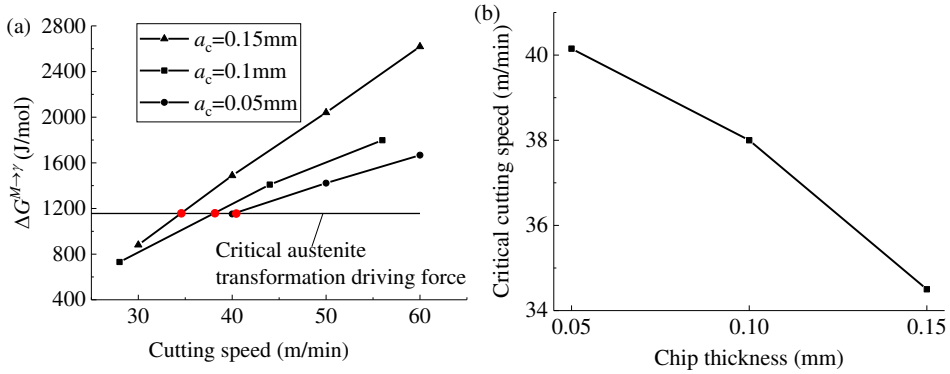

Fig. 8 Prediction of (a) $\Delta G^{M\to\gamma}$, (b) critical cutting speeds of white layer formation at different chip thicknesses (VB = 0 mm, γ_0 = -10°)

4.2 Influence of rake angle on the critical cutting speed of the white layer formation

The tendency of $\Delta G^{M\to\gamma}$ with cutting speed at different rake angles is displayed in Fig. 9(a) (VB = 0 mm, a_c = 0.1 mm). When the tool angle changes from negative rake angle to positive rake angle, the driving force decreases significantly. The tool rake angle has obvious influence on the cutting temperature, stress and strain. When γ_0 changes to positive rake angle, the extrusion and friction between tool rake face and chip are obviously reduced, leading to the decrease in cutting temperature, stress and strain, and thus the decrease in $\Delta G^{M\to\gamma}$. Fig. 9 (b) shows the change rule of critical cutting speed of the white layer formation with the rake angle. When γ_0 changes from

- 10 ° to 10 °, the critical cutting speed increases from 38 m/min to 59.9 m/min, the positive rake angle makes the critical cutting speed of white layer formation increase rapidly.

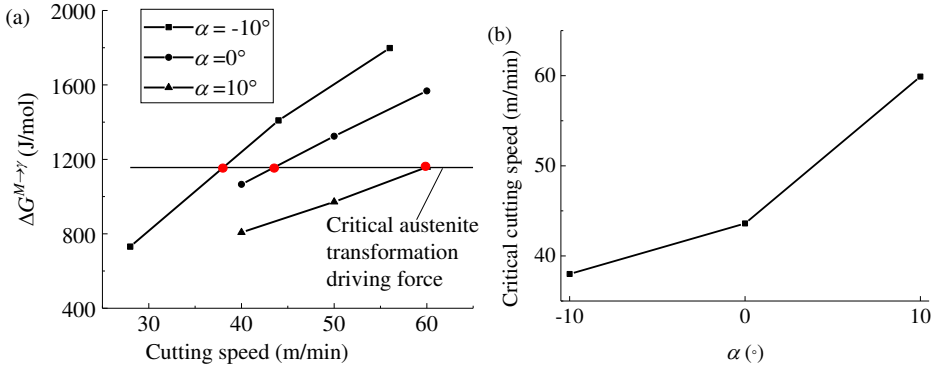

Fig. 9 Prediction of (a) $\Delta G^{M\to\gamma}$, (b) critical cutting speeds of white layer formation at different rake angles (VB = 0 mm, a_c = 0.1 mm)

4.3 Influence of flank wear on the critical cutting speed of the white layer formation

Fig. 10 (a) shows the change of $\Delta G^{M\to\gamma}$ with cutting speed at different levels of flank wear (a_c = 0.1 mm, γ_0 = -10°). At the same cutting speed, $\Delta G^{M\to\gamma}$ increases significantly with flank wear. The cutting heat produced in the hard-cutting process increases significantly with flank wear, providing higher driving force for the austenite transformation. At the same time, the stress and strain energy increase with flank wear, which further promotes the austenite transformation. Influence of flank wear on the critical cutting speed of white layer formation is shown in Fig. 10 (b). When the flank wear is 0.1 mm and 0.2 mm, the critical cutting speeds are 30 m/min and 23.3 m/min, respectively. The flank wear reduces the critical cutting speed of the white layer formation significantly.

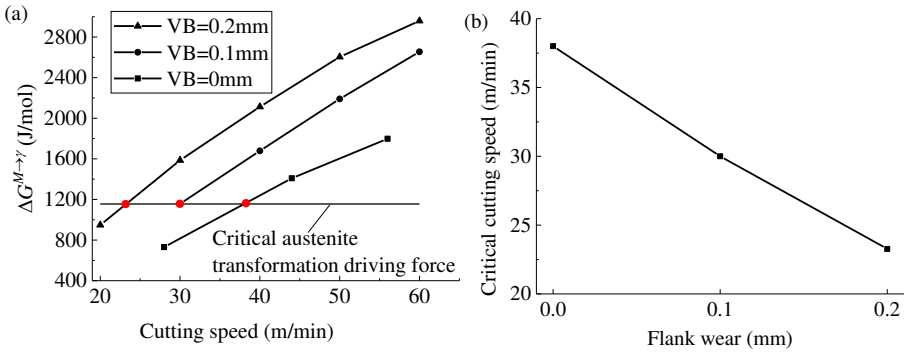

Fig. 10 Prediction of (a) $\Delta G^{M\to\gamma}$, (b) critical cutting speeds of white layer formation at different levels of flank wear (a_c = 0.1 mm, γ_0 = -10°)

5 Conclusion

The models of the austenite transformation driving force and the critical cutting speed of the white layer formation were established. The conclusions can be derived as follows:

(1) The austenite transformation driving force of the white layer in the hard-cutting process was derived mathematically, in which the effects of cutting temperature, stress and strain on the phase transformation driving force were taken into account. It indicates that both the cutting heat and the plastic deformation can provide driving force for austenite transformation.

(2) The prediction model of critical cutting speed of the white layer formation was presented by combining the driving force model with the hard-cutting FE model. The effects of thermal and mechanical factors on the critical cutting speed were considered explicitly. The predicted critical cutting speed is in agreement with the experimental result, which demonstrates the established model is valid in the prediction of the critical cutting speed of phase transformation white layer formation.

(3) On account of the established model, the critical cutting speeds of the white layer formation at different cutting conditions were simulated. The critical cutting speed of the white layer formation decreases with the increase of cutting thickness and flank wear. When the rake angle changes from negative rake angle to positive rake angle, the critical cutting speed increases significantly.

Acknowledgments

This work was supported by the Science and Technology Innovation 2025 Major Project of Ningbo [grant number 2018B10006].

Declarations

a. Funding (information that explains whether and by whom the research was supported)

This work was supported by the Science and Technology Innovation 2025 Major Project of Ningbo [grant number 2018B10006].

b. Conflicts of interest/Competing interests (include appropriate disclosures)

Not applicable

c. Availability of data and material (data transparency)

All data generated or analyzed during this study are included in this published article

d. Code availability (software application or custom code)

The code used in the study are available from the corresponding author on reasonable request.

e. Ethics approval (include appropriate approvals or waivers)

Not applicable

f. Consent to participate (include appropriate statements)

Not applicable

g. Consent for publication (include appropriate statements)

Not applicable

h. Authors' contributions (optional: please review the submission guidelines from the journal whether statements are mandatory)

Not applicable

Reference

1. Li L, Lai D, Ji Q, et al (2021) Influence of tool characteristics on white layer produced by cutting hardened steel and prediction of white layer thickness. Int J Adv Manuf Technol 113:1215–1228. https://doi.org/10.1007/s00170-021-06599-1

2. Hosseini SB, Klement U (2021) A descriptive phenomenological model for white layer formation in hard turning of AISI 52100 bearing steel. CIRP J Manuf Sci Technol 32:299–310. https://doi.org/https://doi.org/10.1016/j.cirpj.2021.01.014

3. Zhang FY, Duan CZ, Sun W, Ju K (2019) Effects of cutting conditions on the microstructure and residual stress of white and dark layers in cutting hardened steel. J Mater Process Technol 266:599–611. https://doi.org/https://doi.org/10.1016/j.jmatprotec.2018.11.038

4. Jouini N, Revel P, Thoquenne G (2020) Influence of surface integrity on fatigue life of bearing rings finished by precision hard turning and grinding. J Manuf Process 57:444–451. https://doi.org/https://doi.org/10.1016/j.jmapro.2020.07.006

5. Zhang F, Duan C, Sun W, Ju K (2019) Influence of White Layer and Residual Stress Induced by Hard Cutting on Wear Resistance During Sliding Friction. J Mater Eng Perform 28:7649–7662. https://doi.org/10.1007/s11665-019-04479-0

6. Cho DH, Lee SA, Lee YZ (2012) Mechanical properties and wear behavior of the white layer. Tribol Lett 45:123–129. https://doi.org/10.1007/s11249-011-9869-4

7. Vyas A, Shaw MC (2000) Significance of the white layer in a hard turned steel chip. Mach Sci Technol 4:169–175. https://doi.org/10.1080/10940340008945704

8. Girisankar S, Omkumar M (2019) Investigation on the hard turning in enhancing the surface reliability by white layer elimination using cbn semi worn-out inserts under shielding gas atmosphere. J Mech Sci Technol 33:2345–2352. https://doi.org/10.1007/s12206-019-0434-7

9. Bosheh SS, Mativenga PT (2006) White layer formation in hard turning of H13 tool steel at high cutting speeds using CBN tooling. Int J Mach Tools Manuf 46:225–233. https://doi.org/10.1016/j.ijmachtools.2005.04.009

10. Chou YK, Evans CJ (1999) White layers and thermal modeling of hard turned surfaces. Int J Mach Tools Manuf 39:1863–1881. https://doi.org/10.1016/S0890-6955(99)00036-X

11. Du J, Liu Z, Lv S (2014) Deformation-phase transformation coupling mechanism of white layer formation in high speed machining of FGH95 Ni-based superalloy. Appl Surf Sci 292:197–203. https://doi.org/10.1016/j.apsusc.2013.11.111

12. Zhang FY, Duan CZ, Wang MJ, Sun W (2018) White and dark layer formation mechanism in hard cutting of AISI52100 steel. J Manuf Process 32:878–887. https://doi.org/10.1016/j.jmapro.2018.04.011

13. Zhang XM, Chen L, Ding H (2016) Effects of process parameters on white layer formation and morphology in hard turning of AISI52100 steel. J Manuf Sci Eng 30:1–6

14. Umbrello D, Jayal AD, Caruso S, et al (2010) Modeling of White and Dark Layer Formation in Hard Machining of AISI 52100 Bearing Steel. Mach Sci Technol 14:128–147. https://doi.org/10.1080/10910340903586525

15. Han S, Melkote SN, Haluska MS, Watkins TR (2008) White layer formation due to phase transformation in orthogonal machining of AISI 1045 annealed steel. Mater Sci Eng A 488:195–204. https://doi.org/10.1016/j.msea.2007.11.081

16. Ramesh A, Melkote SN (2008) Modeling of white layer formation under thermally dominant conditions in orthogonal machining of hardened AISI 52100 steel. Int J Mach Tools Manuf 48:402–414. https://doi.org/10.1016/j.ijmachtools.2007.09.007

17. Duan CZ, Kong W Sen, Hao QL, Zhou F (2013) Modeling of white layer thickness in high speed machining of hardened steel based on phase transformation mechanism. Int J Adv Manuf Technol 69:59–70

18. Zeng H, Yan R, Hu T, et al (2019) Analytical Modeling of White Layer Formation in Orthogonal Cutting of AerMet100 Steel Based on Phase Transformation Mechanism. J Manuf Sci Eng 141:1–7

19. Mohsenzadeh MS, Mazinani M (2020) The Influence of Microstructural Characteristics on Austenite Formation Kinetics in a Plain Carbon Steel. Metall Mater Trans A 51:116–130. https://doi.org/10.1007/s11661-019-05470-z

20. Zhang Y, Li X, Liu Y, et al (2020) Study of the kinetics of austenite grain growth by dynamic Ti-rich and Nb-rich carbonitride dissolution in HSLA steel: In-situ observation and modeling. Mater Charact 169:110612. https://doi.org/https://doi.org/10.1016/j.matchar.2020.110612

21. Marceaux dit Clément A, Hoummada K, Drillet J, et al (2020) Effects of cementite size and chemistry on the kinetics of austenite formation during heating of a high-formability steel. Comput Mater Sci 182:109786. https://doi.org/https://doi.org/10.1016/j.commatsci.2020.109786

22. Guo YB, Sahni J (2004) A comparative study of hard turned and cylindrically ground white layers. Int J Mach Tools Manuf 44:135–145. https://doi.org/10.1016/j.ijmachtools.2003.10.009

23. Kooiker H, Perdahcıoğlu ES, van den Boogaard AH (2020) Combined athermal and isothermal martensite to austenite reversion kinetics, experiment and modelling. Mater Des 196:109124. https://doi.org/https://doi.org/10.1016/j.matdes.2020.109124

24. Adamson A (2012) A textbook of physical chemistry. Elsevier, Amsterdam

25. Lee H G (1999) Chemical Thermodynamics for Metals and Materials. Imperial College press, London

26. Su J (2006) Residual Stress Modeling in Machining Processes. Georg Inst Technol

27. Khodabakhshi F, Kazeminezhad M (2014) Differential scanning calorimetry study of constrained groove pressed low carbon steel: Recovery, recrystallisation and ferrite to austenite phase transformation. Mater Sci Technol (United Kingdom) 30:765–773.